Investigation of the effects of rf fields on superconducting Pb films with quantized resistances*

L. M. Geppert,† R. L. Thomas, and J. T. Chen
Department of Physics, Wayne State University, Detroit, Michigan 48202
(Received 15 January 1976; revised manuscript received 26 January 1977)

An investigtion has been made of the effects of electromagnetic fields of angular frequency $\omega << 2\Delta/\hbar$ on the I-V characteristics of superconducting Pb films with quantized resistances. The effects of both cw ($10\ \text{sec}^{-1} < \omega < 10^9\ \text{sec}^{-1}$) and pulsed ($10^9\ \text{sec}^{-1} < \omega < 10^{10}\ \text{sec}^{-1}$) fields on the different current components of the films have been studied. It is found that the low-frequency response ($\omega \lesssim 10^8\ \text{sec}^{-1}$) is qualitatively different from that of higher frequencies. The low-frequency response can be understood in terms of the time-dependent momentum of the electron pairs which leads to an ac current and also a time-dependent variation of the energy gap. At higher frequencies the experimental results indicate that the time average of the energy gap is strongly power dependent. The observed behavior at high frequencies is consistent with theoretical predictions based on the time-dependent Ginzburg-Landau equations.

I. INTRODUCTION

Superconducting materials are frequently used in applications where strong electromagnetic fields are present. Such applications include transmission lines, superconducting solenoids, rf cavities, and superconducting electronic devices.[1] For this reason, it is becoming increasingly important to understand the effects of high-intensity fields on superconductors. Normally, ground-state electron pairs do not absorb microwaves whose frequency is less than $2\Delta/\hbar$,[2] but the superconducting properties can be affected by the presence of electromagnetic fields if the amplitudes of the fields are sufficiently large.[3,4] For the case of gapless superconductors, there are several theoretical studies which relate the change in the superconducting properties to the intensity of the electromagnetic fields for angular frequencies $\omega << 2\Delta/\hbar$.[5-10] Kulik[5] and Gor'kov and Kopnin (GK)[6] consider the case of thin films. They propose that the type of response is determined by the frequency of the electromagnetic field. At low frequencies, the response is adiabatic, that is, the superconducting energy gap Δ varies with the time-dependent magnitude of the electromagnetic field. The nonadiabatic regime occurs at higher frequencies. In this case, Δ is determined primarily by the intensity of the electromagnetic fields. Kulik estimates that the transition from adiabatic to nonadiabatic behavior occurs in the frequency region $\omega \approx k(T_c - T)/\hbar$ and he has derived expressions for the energy gap and current density in both limits. GK conclude that the behavior can be classified as nonadiabatic in the frequency region $\omega >> 1/\tau$, where τ is the relaxation time of the gap parameter.[11-13] Their calculations pertain only to this regime, but include the effects of finite temperatures and parallel magnetic fields.

We have studied the effects of high-intensity electromagnetic fields with $\omega << 2\Delta/\hbar$ on the I-V characteristics of superconducting Pb films with quantized resistances.[14,15] We have proposed that these quantum-resistance states are produced by a parallel magnetic field $H_{\parallel} \geq H_{c2}$ which generates an S-N-S (*superconductor–normal-metal–superconductor*) structure with N-S (normal-metal–superconductor) phase boundaries parallel to the sample surfaces. The I-V characteristic, which consists of N linear current branches with quantized resistances r_n, is described by the relation

$$I = I_0 + V/r_n \ , \tag{1}$$

where I_0 is the maximum time-average current through the superconducting surface sheaths in the voltage-biased state, and V/r_n is the current in the magnetic-field-induced "normal" lamina due to the coherent flow of bound quasiparticles.[16,17] The current branches terminate at upper cutoff voltages $V_{n\,\max}$ where the total quasiparticle energy in the electric field relative to the Fermi level equals the energy gap of the surface sheaths. The zero-voltage critical current I_c contains two components: I_0 and $I_c - I_0$, where $I_c - I_0$ is the critical current of the normal lamina.

I-V characteristics with voltage steps and multiple current branches have been observed by several investigators.[18] These I-V curves may often be described by Eq. (1) with the modification that, in the general case, I_0 may have a different value for each current branch and the r_n may be functions of I. Skocpol *et al.* have observed step-type I-V characteristics in one-dimensional tin microbridges.[18] They have inter-

preted their results as being due to localized phase slip centers which are in series along the length of the film (i.e., in the direction of current flow) and which become voltage-biased at lower current values than the rest of the film. In relation to Eq. (1), I_0 is then the time-average supercurrent through the phase slip centers and r_n is the sum of the differential resistances of those phase slip centers which generate the nth current branch.

Quantum-resistance states are quite different from phase slip centers in their experimental behavior and the conditions under which they are observed.[15,19] The investigations which are reported in this paper were performed with samples and experimental conditions essentially identical to those used in our studies of the dc properties of quantum-resistance states. Thus, we interpret our present results according to the quantum-resistance-state model.

Since the experimental quantities I_0, $I_c - I_0$, and the V_n max are determined independently, we can study separately the effects of the electromagnetic fields in the surface sheaths and in the normal lamina. From the rf power and frequency dependences of these quantities we have found two distinct types of responses. For frequencies less than 10 MHz our results are in agreement with Kulik's expressions in the adiabatic regime. For frequencies greater than 50 MHz the behavior of our samples appears to be nonadiabatic. We have extended GK's results to obtain an expression for the maximum current density as a function of the time-average electromagnetic field intensity inside the film. When we consider the surface sheaths and the central lamina as separate thin films, the power dependence of the maximum current in each region agrees well with the derived relationship.

II. EXPERIMENTAL DETAILS

Our samples were prepared by thermal evaporation of high-purity Pb pellets (99.9999%, A. D. McKay, Inc.) at a pressure of approximately 10^{-6} Torr. Several samples were evaporated onto quartz substrates and others were prepared on glass. However, the poor thermal conductivity of the glass caused the samples to burn out when they were driven normal at large critical current values. No damage resulted to the films on quartz substrates under similar conditions.

More than a dozen samples have been studied. Two of them, samples 1 and 2, have been investigated thoroughly. Sample 1 was evaporated onto an X-cut single-crystal quartz rod ($\frac{1}{2}$-in. diameter by $1\frac{1}{2}$-in. length), while sample 2 was evaporated onto a thin quartz substrate. The thickness of the films (3500 Å) and the rate of evaporation (30 Å/sec) were controlled by a quartz-crystal oscillator (Sloan Omni II with sensing head model 103-752). After evaporation, the films were coated with a thin layer of Kodak Ortho Resist for protection. The width and length of our samples were 0.28 and 2.02 mm, respectively. The resistivity ratios, $R(300\text{ K})/R(4.2\text{ K})$, were 107 for sample 1 and 56 for sample 2.

Sample 2 was mounted on a copper block and held in place by a thin layer of Apiezon N-type vacuum grease. Sample 1 was held in place by a brass clamp. The samples were directly immersed in liquid helium. The temperature was lowered from 4.2 K by pumping above the helium bath and its value was determined by monitoring the helium vapor pressure.

The usual four-terminal arrangement and a constant-current source were used to measure the I-V characteristics. Time-dependent voltages were measured on an oscilloscope or on a PAR boxcar integrator model 160. The electromagnetic fields were coupled to the sample either directly by soldering the rf leads onto the film, or inductively, by placing a loop of wire in proximity to the sample. It was found that inductive coupling induced a far weaker response than direct coupling. For cw in the frequency range 10–500 MHz, the maximum rf voltage across the output terminals of the rf generator was 20 V. For pulsed rf (0.25–1.2 GHz) the maximum peak voltage was 1.0 kV. Due to the impedance mismatch and the lack of understanding of the nature of the coupling between the sample and the leads, it was not possible to determine the actual magnitude of the rf fields inside the film. However, we believe that they must be several orders of magnitude smaller. Our measurements of power dependence are presented in terms of arbitrary units proportional to the square of these rf voltages. All the experimental curves presented in this article were obtained with the rf leads directly soldered to the films.

III. RESULTS AND DISCUSSION

A. Low frequency (<10 MHz)

As shown in Fig. 1(b), application of electromagnetic fields in the range of frequencies less than 10 MHz, reduces the upper critical currents (e.g., I_c and I_{c1}^{+}), while enhancing the lower critical currents (e.g., I_{c1}^{-}) by an equal amount, where I_{c1}^{+} and I_{c1}^{-} are the upper and lower critical currents of the first current branch. This behavior can be understood simply in terms of the superposition of dc current and the ac current induced by the electric field. Although we measure only the dc component I, the total current is actually $I_T = I + I_{ac} f(t)$, where $f(t)$ is a periodic function. The sample switches to $n = 1$ when $I_T \geq I_c$ and to $n = 2$ when $I_T \geq I_{c1}^{+}$; similarly it switches back to the zero-voltage branch when $I_T \leq I_{c1}^{-}$. Thus, the measured values of the upper critical currents are reduced by the maximum amplitude of the ac current I_{ac},

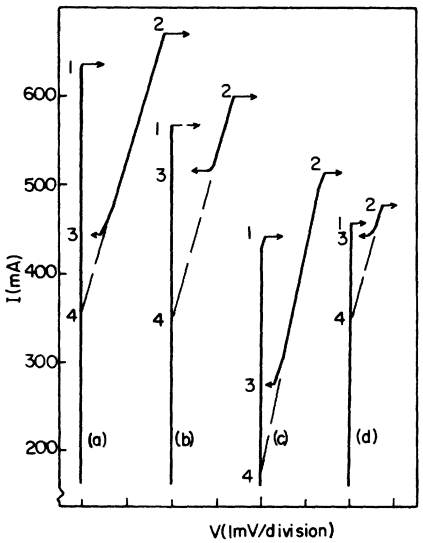

FIG. 1. Changes in the I-V characteristic of a Pb film due to electromagnetic fields: (a) zero power; (b) 10-kHz cw; (c) 300-MHz cw; (d) 300-MHz pulsed. The numbers correspond to the following quantities: $1-I_c$; $2-I_{c1}^{+}$; and $V_{1\max}$; $3-I_{c1}^{-}$; $4-I_o$.

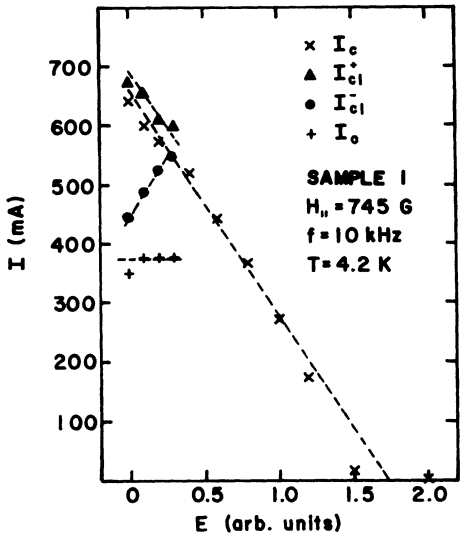

FIG. 2. Various current components as functions of electric field amplitude at 10 kHz. I_c—zero-voltage upper critical current; I_{c1}^{+}—upper critical current of first current branch; I_{c1}^{-}—lower critical current of first current branch; I_o—extrapolation of linear current branches to zero voltage.

while the lower critical currents are enhanced by the same amount. The sample can be dc biased on $n=1$ only for $I_{ac} < \frac{1}{2}[I_{c1}^{+}(0) - I_{c1}^{-}(0)]$, where $I_{c1}^{+}(0)$ and $I_{c1}^{-}(0)$ are the values of these quantities when $I_{ac}=0$. Within this range, our results indicate that I_0 and r_1 are unaffected by the ac current. For $I_{ac} > \frac{1}{2}[I_{c1}^{+}(0) - I_{c1}^{-}(0)]$, the I-V characteristics become washed out as the ac current cycles the sample through several different current branches. $n=1$, I_{c1}^{+}, I_{c1}^{-}, and I_0 can no longer be identified. I_c remains a measurable quantity, and is plotted as a function of E in Fig. 2 for a frequency of 10 kHz, where E is the maximum amplitude of the applied electromagnetic field.[20] Also shown, in the low-amplitude region, are I_{c1}^{+}, I_{c1}^{-}, and I_0. Assuming that the impedance of our circuit is power independent, $E \propto I_{ac}$ so that $I_c(0) - I_c \propto E$. It can be seen from Fig. 2 that all quantities display the expected behavior.

For an oscillatory electric field in the film $E(t) = E_0 \cos\omega t$, where ω is in the adiabatic regime, Kulik has derived the following dimensionless equations for the order parameter $\Delta(t)$ and the current density $j(t)$:

$$\Delta^2(t) \approx \begin{cases} f'(t) & \text{for } f'(t) > 0 \ , \\ 0 & \text{for } f'(t) < 0 \ , \end{cases} \tag{2}$$

where

$$f(t) = \int_0^t [1 - (q + z\sin\omega t)^2]\, dt \ , \quad f'(t) = \frac{df}{dt} \ ,$$
$$j(t) = (q + z\sin\omega t)\Delta^2(t) + \gamma\omega z \cos\omega t \ , \tag{3}$$

where q is the dc transport momentum normalized to the inverse of the coherence length ξ, $z = \sqrt{2}E_0/E_{cr}$, and E_{cr} is the amplitude of the electromagnetic field at which Δ^2 vanishes for $q=0$. $\gamma = 2\lambda_L^2\epsilon_0/\delta_{sk}^2\omega$, where λ_L is the London penetration depth, ϵ_0 is the permittivity of free space and δ_{sk} is the skin depth in the normal state. Apparently, the cosine term in the expression for $j(t)$ is the in-phase current of the normal electrons. The coefficient of this term is very small for $\hbar\omega \ll k(T_c - T)$. q is related to the momentum of the superconducting electrons in a dc transport current and $z\sin\omega t$ is their momentum in the ac current generated by the electromagnetic field. In determining both the total momentum and the density of superconducting electrons, equal roles are taken by q and $z\sin\omega t$. Thus the critical current density is independent of their relative magnitudes, which means simply that as z increases, the dc current required to drive the film into the resistive state decreases proportionally. In fact, it is the time-dependent momentum of the electron pairs in response to the electromagnetic field which is actually responsible for the adiabatic variation of Δ. Note that because the time-dependent momentum of the electron pairs is 90° out of phase with the electric field, Δ has its minimum value when $E(t)=0$ and the time-dependent momentum of the electron pairs is maximum.

B. High frequency (50 MHz–1.2 GHz)

1. Continuous wave

In describing the response of superconducting thin films to rf fields, GK decompose Δ^2 into two parts

such that $\Delta^2 = \langle\Delta^2\rangle + (\Delta^2)_1$, where $\langle\Delta^2\rangle$ is time independent and $(\Delta^2)_1$ varies with the same frequency as the rf field. In the nonadiabatic limit, $(\Delta^2)_1 \ll \langle\Delta^2\rangle$ so that Δ^2 is essentially a time-independent function of rf intensity. These authors state that the transition from the adiabatic to the nonadiabatic regimes occurs at an angular frequency $\omega \approx \tau^{-1} \approx 10^8 - 10^9$ sec^{-1}, where τ is the relaxation time of the gap parameter. This range of τ is the same as that calculated by Woo and Abrahams[12] for the reduced temperature region $0.9 < t < 0.99$. The gap relaxation time has also been studied theoretically by other investigators. Lucas and Stephen[11] find that for $\Delta \ll kT$ the order of magnitude of the gap relaxation time is $(10^8 T^3)^{-1}$ sec. Schmid[13] has calculated the gap relaxation time in both the clean and dirty limits and for conditions of both large and zero dc currents. We believe that the dirty limit applies to our case since our calculated mean-free path at 4.2 K is 1750 Å, which is just half the film thickness. The large-dc-current case also applies since we are studying the changes in the I-V characteristic due to the rf field, and these changes are observed when the current is near its critical value. For dirty samples transporting large dc currents Schmid finds

$$\tau = \frac{27\pi^5}{640}\left[\frac{7\zeta(3)}{8}\right]^2 \frac{\hbar}{kT_c}\left(\frac{T_c}{T_c - T}\right)^5 \frac{q_m{}^6/q^6}{(1 - \frac{1}{3}q^2/q_m{}^2)^2}\ , \tag{4}$$

where q_m is the center-of-mass momentum of the Cooper pairs for which the current is maximum. However, since Schmid's calculation does not include a magnetic field and our measurements are taken in a parallel field near 740 G, Eq. (4) cannot be strictly applied to our case. It is not clear from Eq. (4) precisely what effect the magnetic field should have on the gap relaxation time. However, Lucas and Stephen's calculations show that τ diverges as the gap parameter goes to zero [Eq. (21) of Ref. 11]. Application of a magnetic field reduces the gap parameter and thus should increase its relaxation time. With this in mind, we propose as a first-order correction that the value of T_c in Eq. (4) be modified to take the magnetic field into account. In place of a T_c of 7.2 K, we substitute the temperature T_c^* at which Pb becomes normal in a parallel field of 740 G, which is the temperature at which $H_{c3} = 740$ G. We calculate T_c^* by using the parabolic dependence of $H_c(T)$ on T and the relationship $H_{c3}(T) = 1.695[\sqrt{2}\kappa H_c(T)] = 1.695 H_{c2}(T)$. At 4.2 K we find $H_{c2} = 740$ G so that $H_{c3}(4.2\text{ K}) = 1254$ G. Neglecting any temperature variation of κ between 4.2 K and T_c^* and taking the ratio $H_{c3}(T_c^*)/H_{c3}(4.2\text{ K}) = 740\text{ G}/1254\text{ G}$ gives a value of $T_c^* = 5.6$ K. Using this value for T_c in Eq. (4) and setting $q = q_m$ gives a relaxation time of $\tau = 4.5 \times 10^{-8}$ sec. On the other hand, if we neglect the magnetic field and simply use $T_c = 7.2$ K in Eq. (4), we obtain $\tau = 0.27 \times 10^{-8}$ sec.

Experimentally, the relaxation time of the Cooper pair density in Sn has been investigated by Peters and Meissner.[21] They find good agreement with Schmid's calculation for clean films, with a relaxation time $\tau > 10^{-9}$ sec near T_c. Schuller and Gray have studied the relaxation time of the gap parameter in Al.[22] They find relaxation times ranging from 10^{-7} to 10^{-6} sec near T_c. Both studies confirm the theoretically predicted divergence of τ as $T \to T_c$.

Experimentally we observe a qualitative change in the response of our samples to the rf fields in the frequency range 10–50 MHz. Above this frequency region, evidence of cycling disappears. I_{c1}^- no longer increases with increasing rf amplitude. Instead, all quantities decrease with increasing rf power [Fig. 1(c)]. We interpret this frequency region as the one proposed by GK to separate adiabatic from nonadiabatic behavior. This would suggest a gap relaxation time of approximately 2×10^{-8} sec, which is in the range predicted theoretically and observed experimentally.

The response of I_{c1}^+, I_c, I_{c1}^-, and I_0 to increasing rf amplitude, E, for a frequency of 300 MHz is shown in Fig. 3. These data are representative of our results in the frequency range 50–500 MHz.

Gor'kov and Kopnin have obtained an expression for the time variation of the gap parameter in the presence of a microwave field of slow varying amplitude and a constant transport current. By setting the time variation equal to zero, we obtain the following steady-state expression for Δ:

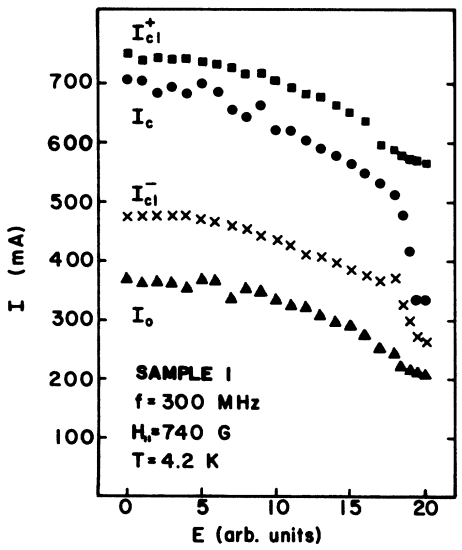

FIG. 3. Various current components as function of rf amplitude at 300 MHz.

$$\Delta^2 = 1 - E_0^2/E_{cr}^2 - q^2/(1-H) \ , \tag{5}$$

where E_0^2 is the rf intensity inside the film and H is the reduced parallel magnetic field normalized to $H_{c\|}$. q and E_{cr} have been defined in the previous section. In Eq. (5), Δ is normalized to its zero-power zero-current value at the applied magnetic field. The constant transport current is specified by

$$j = a(1-H)\Delta^2 q \ , \tag{6}$$

where a is a dimensionless constant. Following Kulik's procedure, we substitute for Δ^2 and maximize j with respect to q to obtain

$$j_{max} = (2a/3\sqrt{3})(1-H)^{3/2}(1-E_0^2/E_{cr}^2)^{3/2} \ . \tag{7}$$

The suitability of a direct application of GK's theory to our measurements must be examined. GK's calculations were done for a thin film, which implies that both the energy gap and the magnetic field are independent of position in the direction normal to the film surface. For our sample, neither of these conditions is fulfilled. The energy gap is much larger in the surface sheaths and the magnetic field penetrates only into the normal lamina. In order to apply their theory, we assume that the surface sheaths and the normal lamina can be treated as separate thin films. We also assume that in the surface sheaths Δ is constant, and in the normal lamina Δ is comparatively small and H is constant across its thickness. The absence of H in the surface sheaths is not too severe a problem. The purpose of the magnetic field in GK's theory is to render the film gapless so that the time-dependent Ginzburg-Landau equations may be expanded in powers of Δ.[7] However, the surface sheaths are, in fact, gapless superconductors.[23] For reasons described below, we think it is reasonable to assume that the functional dependence of Δ and j on E_0 should not depend upon the mechanism responsible for the gapless behavior. First, the equations upon which GK base their calculations have the same form as those used for other types of gapless superconductors. GK point out that their differential equation for Δ is analogous to the one obtained in Ref. 8 for superconductors with paramagnetic impurities. Second, Kulik[5] whose calculations were made for the paramagnetic case also believes that the situation should be analogous for all gapless superconductors.

In order to compare our experimental results with Eq. (7) we take the ratio

$$\frac{j_{max}(E_0)}{j_{max}(0)} = \frac{I_{max}(E_0)}{I_{max}(0)} = \left(1 - \frac{E_0^2}{E_{cr}^2}\right)^{3/2} \ , \tag{8}$$

with $I_{max} = I_0$ for the surface-sheath critical current and $I_{max} = I_c - I_0$ for the critical current of the normal lamina. Figure 4 is a plot of $I_0(E)/I_0(0)$ vs $(1-E^2/E_{cr}^2)^{3/2}$ and Fig. 5 is a similar plot for $I_c - I_0$.

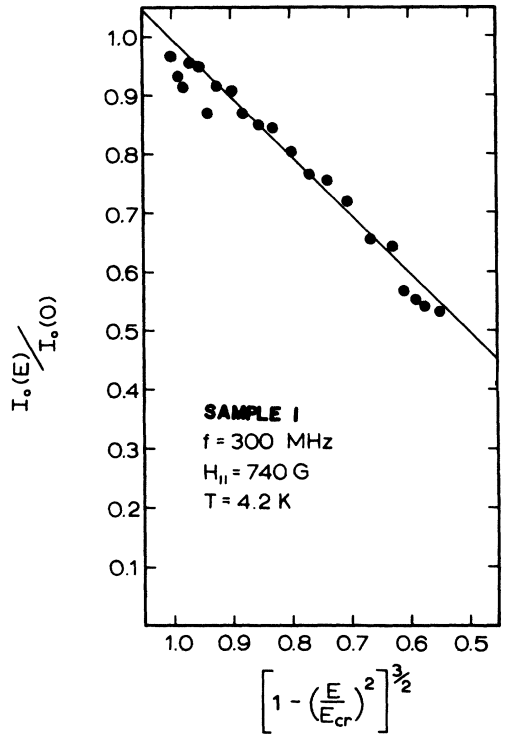

FIG. 4. I_0 as a function of rf intensity at 300 MHz. Solid line is theoretical curve.

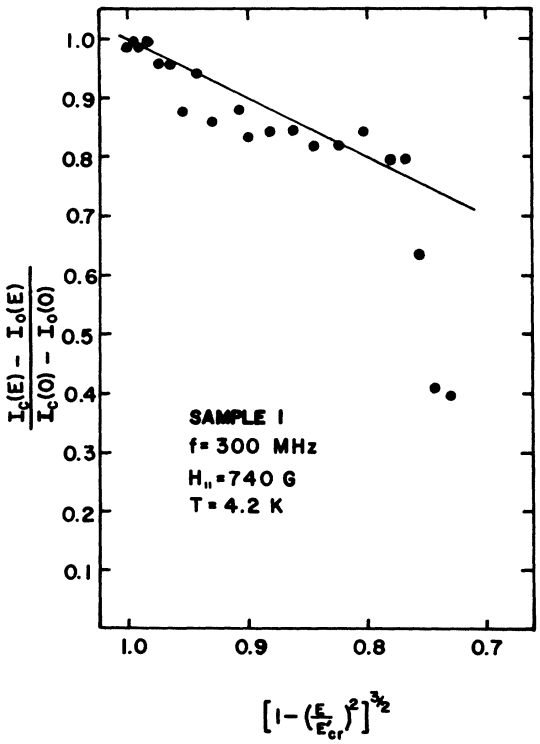

FIG. 5. $I_c - I_0$ as a function of rf intensity at 300 MHz. Solid line is theoretical curve.

In each case the value of E_{cr} used is the one which gives the best fit to Eq. (8). We find that the value of E_{cr}' used for the normal lamina is larger by a factor of 1.3 than E_{cr} used for the surface sheaths.

Since the surface sheath and central regions are in different states (as discussed in the preceding paragraph), we should not expect the critical rf amplitudes F_{cr} and E_{cr}' to be necessarily the same. For the same reason, the actual intensity of the rf fields, E_0^2, may be different in the two regions. This would also lead to different critical values of the applied rf field.

In Fig. 5, we note that there is a point in the power dependence at which the value of $I_c - I_0$ drops abruptly. (The I-V traces taken with power levels near this point were quite unrepeatable, showing sometimes the low-power and other times the high-power behavior.) With the exception of $I_c\dagger$, indications of a sharp transition are observed for all the measured quantities. For rf intensities lower than the transition point, our data fit the theoretical curves quite well. However, it must be borne in mind that since we are plotting the various components as functions of applied rf field, our comparison with Eq. (8) is only meaningful when the transmission coefficient $(E_0/E)^2$ is independent of rf intensity. GK's results indicate that, to a good approximation, this is the case for low levels of intensity (see Fig. 1 of Ref. 6). Moreover, they predict that at some value of intensity, which depends on the parameters a, H, and ω, there is an abrupt and possibly discontinuous increase in the transmission coefficient. This may account for the transition which we observe in our measurements. Similar power dependence for the transmission coefficient has been observed experimentally in Sn films.[24]

The dependence of $V_{1\,max}$ on rf intensity may also be compared with predictions based on GK's theory. $V_{1\,max}$ is given by[15]

$$V_{1\,max} = \frac{L\pi}{k_F e d^2}(1-\alpha)\left[\Delta - \frac{h^2}{8md^2}(1-\alpha)^2\right], \quad (9)$$

where, for our measurements, $\alpha = 0$. L is the length of the sample, d is the thickness of the normal lamina, and $\hbar k_F$ is the Fermi momentum. The second term in large parentheses is much smaller than Δ, the energy gap of the surface sheaths. For the intensity region where $E_0 \propto E$,

$$\frac{V_{1\,max}(E)}{V_{1\,max}(0)} \approx \frac{\Delta(E)}{\Delta(0)} = \left[1 - \left(\frac{E}{E_{cr}''}\right)^2\right]^{1/2}. \quad (10)$$

This dependence is shown in Fig. 6. Again, a different value of E_{cr} had to be used in order to obtain the proper slope. Its relationship to the value used for I_0 is $E_{cr}''/E_{cr} = 0.69$. One possible reason for this difference is that I_0 is a measure of the average value of Δ in the surface sheaths, whereas $V_{1\,max}$ probes its

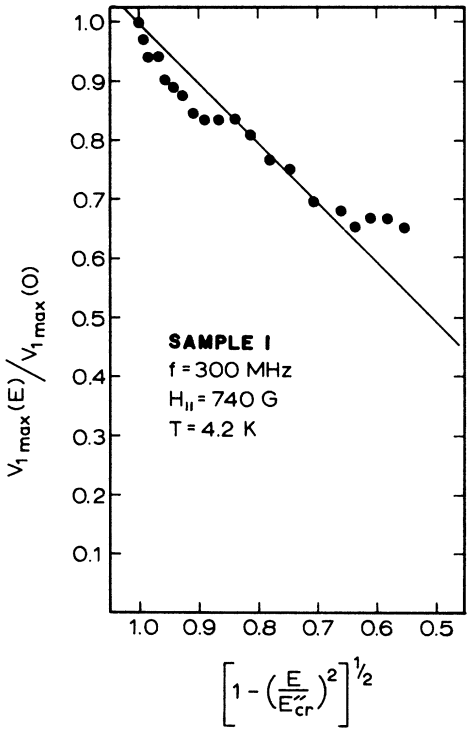

FIG. 6. $V_{1\,max}$ as a function of rf intensity at 300 MHz. Solid line is the theoretical curve.

value at the N-S interface. The energy gap at the interface may be more sensitive to perturbations than Δ in the interior of the surface sheaths or of the normal lamina.

Our analysis was carried out with the assumption that the thickness of the normal lamina d remains constant. However, our measurements of r_1 for sample 1 indicate that d increases slightly with increasing E (Fig. 7). Since $r_1 \propto 1/d^3$,[15]

$$\frac{d(E)}{d(0)} = \left[\frac{r_1(0)}{r_1(E)}\right]^{1/3}. \quad (11)$$

If we incorporate this correction into Eqs. (8) and (10) we obtain

$$\frac{I_0(E)}{I_0(0)} = \frac{D - d(0)}{D - [r_1(0)/r_1(E)]^{1/3} d(0)}\left[1 - \left(\frac{E}{E_{cr}}\right)^2\right]^{3/2}, \quad (12)$$

$$\frac{I_c(E) - I_0(E)}{I_c(0) - I_0(0)} = \left[\frac{r_1(0)}{r_1(E)}\right]^{1/3}\left[1 - \left(\frac{E}{E_{cr}'}\right)^2\right]^{3/2}, \quad (13)$$

$$\frac{V_{1\,max}(E)}{V_{1\,max}(0)} = \left[\frac{r_1(E)}{r_1(0)}\right]^{2/3}\left[1 - \left(\frac{E}{E_{cr}''}\right)^2\right]^{1/2}, \quad (14)$$

where D is the total film thickness. The correction

factors in Eqs. (13) and (14) may be obtained directly from the data. For Eq. (12), assumptions concerning the values of D and $d(0)$ are required. Taking $D = 3500$ Å and $d(0) = 2100$ Å, and renormalizing the curve for $I_0(E)/I_0(0)$ yields a value of E_{cr} which is larger than the previous value by a factor of 1.22. Renormalizing the other two curves yields new critical amplitude ratios of $E_{cr}'/E_{cr} = 0.95$ for $I_c - I_0$, and $E_{cr}''/E_{cr} = 0.69$ for $V_{1\,max}$.

Due to the power limitations of our rf generator, data in the power region $E > 0.5\ E_{cr}$ could not be obtained. But even if this data were available it would not follow Eq. (8) because of changes in the transmission coefficient at high-power levels. Although this parametrized fit is not necessarily unique, the experimental behavior in the power region studied is consistent with the theoretical model.

2. *Continuous wave with power modulation*

When the sample is biased on any current branch with finite voltage, and the rf intensity is modulated at audio frequency, a corresponding modulation of the sample voltage is observed on the oscilloscope. This response is due to the dependence of I_0 on rf power. It can be seen from Fig. 1(b) that as the rf power increases and I_0 decreases, the entire $n = 1$ branch is shifted downward. Comparing the zero power [Fig. 1(a)] and rf power [Fig. 1(c)] traces it is observed that there is a range of current values for which the sample can be biased on the $n = 1$ branch of either trace. For a bias current within this range, the sample voltage is larger with the rf power applied. Thus when the rf power is modulated, the sample voltage also varies between two limiting values. With the film biased on the zero voltage branch, no modulation of the sample voltage is observed. This is reasonable since, in this case, the voltage is the same for both zero and high rf intensities. These observations are in agreement with the predictions of GK. They have determined that when the microwave power is slowly varied, the energy gap follows the variation adiabatically.

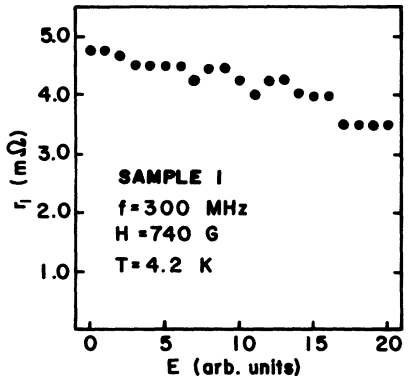

FIG. 7. r_1 as a function of rf amplitude at 300 MHz.

3. *Pulsed rf*

In this portion of the experiment, rf pulses of 0.7-μsec duration and 1-kHz repetition frequency were applied to the sample. The response of the I-V characteristic is shown in Fig. 1(d). In this case the upper critical currents (I_c and the I_{cn}^{+}) are reduced as rf power is increased. However, the pulses do not affect the values of I_{cn}^{-}, r_n, or I_0. Shown in Fig. 8 are plots of I_c and I_{c1}^{+} vs E^2. The initial decline is rapid, but both quantities level off to a constant value at higher power. The leveling-off occurs when the upper critical currents are reduced to the point where they coincide with the returning trace. This type of behavior can be best understood in terms of the results for cw modulation. While the pulse is on, all quantities in the I-V characteristic are actually suppressed, just as in the case of cw. Thus the sample cannot be stably biased on any current branch when the dc current exceeds the peak-power critical current of that branch. Consequently, the measured values of I_c and I_{c1}^{+} are properties of the peak power response. On the other hand, when the sample is biased on a current branch, the voltage may actually increase over the duration of the pulse. However, the X-Y recorder does not respond to pulses of such short duration, and so the dc voltages and resistances measured are properties of the zero-power I-V characteristic. Consequently, the extrapolation of the current branches to zero voltage, i.e., I_0, is the same as the zero-power value. For the same reason, the responses of I_c and I_{c1}^{+} appear to saturate at high power. In reality, they may be reduced far below the returning trace. However, when the sample is biased below $I_{1\,min}$, voltage develops only while the pulse is on. Again, this short voltage pulse is not detected by the X-Y recorder and so the sample ap-

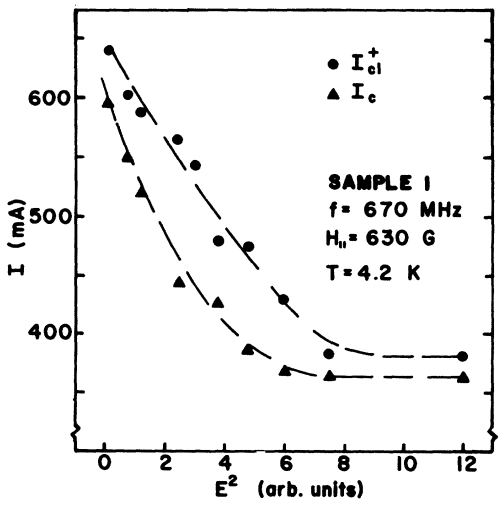

FIG. 8. I_{c1}^{+} and I_c as functions of pulsed rf intensity at 670 MHz.

pears to remain stably biased on the zero-voltage branch. Observation of the sample voltage versus time on the oscilloscope verifies that voltage does develop over the pulse duration while the sample is biased by a constant current.

The time-dependent voltages were also studied by using a boxcar integrator. Figure 9 shows the time-dependent voltage for several different values of dc bias current I_{dc} and dc bias voltage V_{dc}. The origin for each curve has been offset for clarity of presentation. The initial rise of voltage occurs over a period of approximately 0.7 μsec, which is the duration of the rf pulse. The decay time back to the initial voltage depends upon the value of I_{dc}. For low-bias currents the voltage may return to zero long before the film has returned to equilibrium. For most of the traces taken in both parallel and perpendicular fields, the time required for the voltage to decay to half of its peak value is approximately 0.5 μsec. This is about an order of magnitude larger than the gap relaxation time and may be due to the time constant of the circuit. The voltage decay curve for the 600 mA trace in Fig. 9 is somewhat broader than the others and, in addition, appears to be structured. The reason for this lies in the fact that the sample is dc biased in the region where the bound-state current branches are observed. In the I-V characteristics of films with quantized resistances, the return to zero voltage occurs in a series of voltage steps, each of which is associated with one of the bound-state current branches. The total relaxation process is thus a sequence of transitions in which the quasiparticles relax to successively lower bound states. Consequently, the total relaxation time is the sum of the times required for each transition.

The magnitude of the pulse ΔV is determined by I_{dc}. As shown in Fig. 9, for sample 2, no voltage pulse develops if I_{dc} is less than 300 mA. For $I_{dc} > 300$ mA, ΔV becomes larger as I_{dc} increases, reaching a maximum just below I_{c1}^{-}. Above I_{c1}^{-}, a dc voltage develops and ΔV begins to decrease, reaching a minimum when the sample is biased on the normal branch (top curve). A voltage pulse should not be observed when I_{dc} is less than the peak-power critical current I_{cp}. Thus, I_{cp} (300 mA in this case) can be determined by the value of I_{dc} at which a pulse first appears. Figure 10 shows plots of ΔV vs I_{dc} for several different values of rf amplitude E. For the lowest amplitude, $E = 0.3$, a pulse is only observed for $I_{dc} \geq 700$ mA. The next higher amplitude, $E = 0.7$, indicates $I_{cp} \approx 300$ mA. For $E = 1.0$, $I_{cp} \approx 0$ mA. Further increase of power has little effect on ΔV; the values for the two highest amplitudes, $E = 1.0$, and $E = 2.0$, are very close. The sum of V_{dc} and ΔV gives the total peak-power voltage V_p across the sample. Thus by plotting V_p vs I_{dc} the peak-power I-V characteristic can be obtained. Figure 11 contains two such

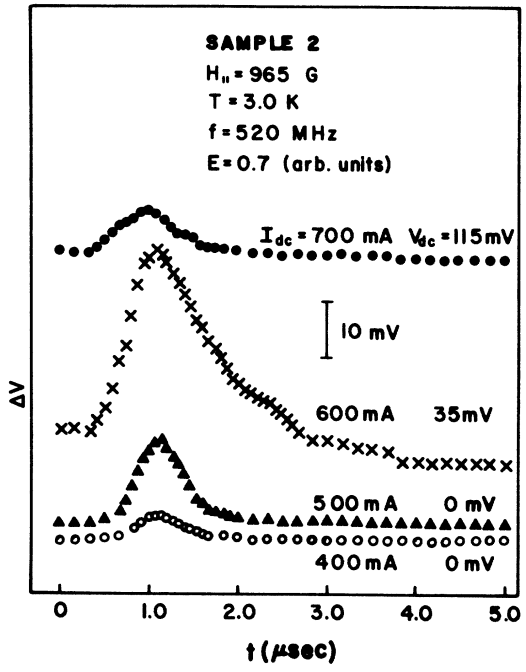

FIG. 9. Time-dependent voltage of sample in pulsed rf field and parallel magnetic field for several values of dc bias current. The origin of each curve is offset along the ΔV axis. The voltage scale is indicated by the marker in the figure.

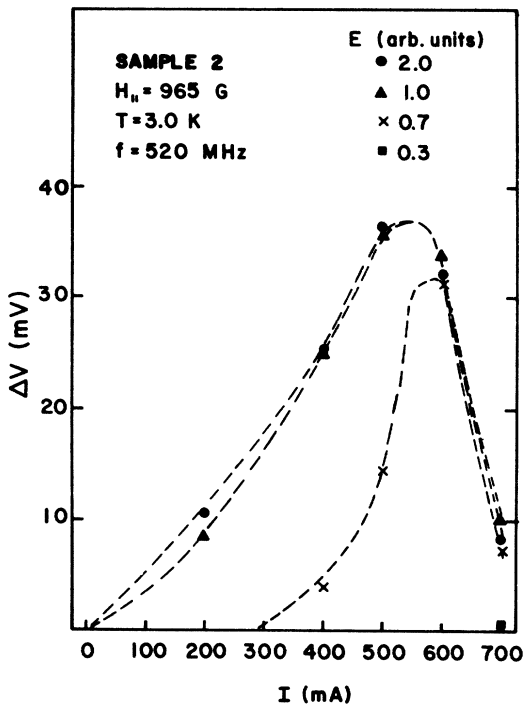

FIG. 10. Time-dependent voltage as a function of dc bias current for several values of rf amplitude and a parallel magnetic field of 965 G.

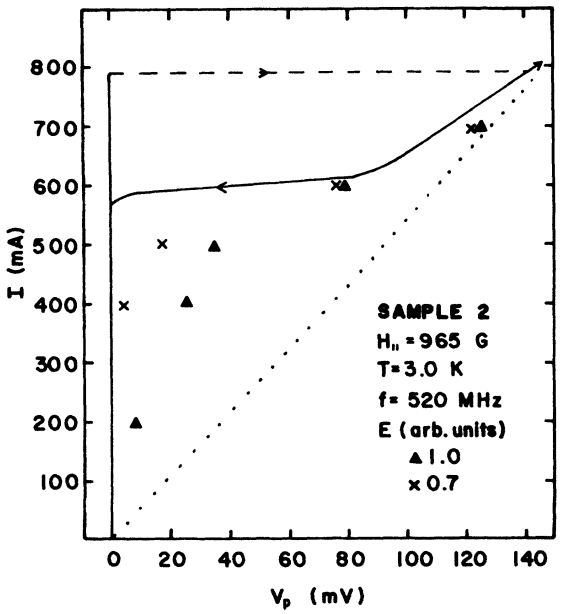

FIG. 11. dc bias current vs peak-power voltage, $V_{dc}+\Delta V$, in a parallel magnetic field. Solid lines indicate the zero-power I-V curve. Dotted line is the normal trace.

plots, for rf amplitudes $E=0.7$ and $E=1.0$. The solid lines indicate the zero-power I-V characteristic. Also shown is the normal state trace (dotted line). The value of V_p is limited by the voltage which would develop if the sample were driven completely normal. For high levels of I_{dc}, the voltage difference between V_{dc} and the normal trace is quite small. This explains why ΔV diminishes for large values of I_{dc}. We have extended our measurements up to a frequency of 1.2 GHz. We find that although the response is weaker, the behavior is similar to that presented here.

4. *Heating effects*

The significance of heating effects in a film depends largely on the type of substrate. The thermal conductivity of the glass commonly used for substrates is very poor. Consequently, the normal-state I-V characteristics of Pb films deposited on glass substrates frequently show curvature, indicating that the resistivity is increasing as the power is increased. The increase in resistivity is due to the rise of the film temperature, which is caused by inadequate removal of heat. If the film is immersed in liquid helium, almost all of the heat must be removed by the helium bath. So if the Joule heating exceeds the critical value[25] for heat flow from a metal film to the surrounding liquid helium, there will be thermal runaway due to the boiling and vaporization of the helium. In contrast, we have found experimentally[26] that the I-V characteristics of Pb films deposited on quartz substrates remain linear even at large-current and -voltage values. This indicates that the temperature does not increase significantly. We have also found that the critical value of Joule heating required for thermal runaway is at least an order of magnitude larger than the corresponding value for films on glass substrates. Since the films used in this experiment were deposited on quartz substrates and did not display any of the heating effects mentioned above, we believe that the thermal conduction properties of the system were sufficient to maintain the temperature of the film at a constant value during the cw measurements. Furthermore, if heating were the dominant factor in the cw experiment, we would expect that the frequency dependence would be influenced by the power level of the rf fields. However, we found that the crossover frequency remained the same even if the rf power was varied by two orders of magnitude. We wish to emphasize that the crossover frequency was determined by the qualitative change in the power dependence of the I-V curves. This change is due to the disappearance above the crossover frequency of cycling of the I-V curves due to the superposition of dc and ac current. We do not believe that heating effects can account for these observations.

Another way of determining if a film is temporarily heated to a higher temperature by the combination of dc and rf currents is to examine the "normal" branch of the I-V characteristic. The normal branch in the I-V characteristic of a film in the superconducting state is usually different from the corresponding I-V characteristic of the same film in the normal state. In the former case, the normal branch does not extrapolate to zero current at zero voltage. Experimentally, we have found that the intercept at zero voltage depends on the temperature and the magnetic field. A change in the temperature of the film in the presence of rf fields will cause the intercept at zero voltage to shift. For the case of cw experiment, we did not observe such a shift. Thus, we can conclude that heating is not a significant factor in our measurement of cw power dependence. In the measurement with pulsed rf fields where the power is a factor of 10^2 higher than the cw case, we did observe a slight increase in voltage over the pulse duration when the film was biased on the normal branch (uppermost curve of Fig. 9). So our observations of the effects of high-power rf pulses may be due to a combination of rf effects and heating.

IV. CONCLUSION

We have used quantum-resistance states to study the nonlinear electrodynamic effect in superconducting films. Because we can experimentally distinguish the surface-sheath currents from those of the central lamina, we can study separately their responses to the

electromagnetic field. We have found that for frequencies less than 10 MHz, our experimental results can be understood in terms of the time-dependent momentum of the electron pairs which leads to an ac current and also to an adiabatic variation of the energy gap. In the nonadiabatic regime, our results for both surface sheaths and normal lamina are consistent with the theoretical predictions of Gor'kov and Kopnin, derived for gapless thin films. The transition from adiabatic to nonadiabatic behavior occurs at a frequency of approximately 5×10^7 Hz, yielding a gap relaxation time of 2×10^{-8} sec. This is within a range of values which has been predicted theoretically and observed experimentally by other investigators.

---

*Work supported by NSF Grant No. DMR 74-02616-A01 (formerly No. GH-43837).

†Present address: IBM Thomas J. Watson Research Center, Yorktown Heights, N.Y. 10598.

[1]"Applied Superconductivity Conference 1974," IEEE Trans. Mag. MAG-11, (1975).

[2]D. M. Ginsberg and L. C. Hebel, in *Superconductivity,* edited by R. D. Parks (Marcel Dekker, New York, 1969), Chap. 4.

[3]A. G. Wyatt, V. M. Dmitriev, W. S. Moore, and F. W. Sheard, Phys. Rev. Lett. 16, 1166 (1966).

[4]L. M. Geppert, R. L. Thomas, and J. T. Chen, in *Proceedings of the Fourteenth International Conference on Low-Temperature Physics, Helsinki, 1975,* edited by M. Krusius and M. Vuorio (North-Holland–American Elsevier, New York, 1975), Vol. 2, p. 215.

[5]I. O. Kulik, Zh. Eksp. Teor. Fiz. 57, 600 (1969) [Sov. Phys.-JETP 30, 329 (1970)].

[6]L. P. Gor'kov and N. G. Kopnin, Zh. Eksp. Teor. Fiz. 59, 234 (1970) [Sov. Phys.-JETP 32, 128 (1971)].

[7]L. P. Gor'kov and G. M. Eliashberg, Zh. Eksp. Teor. Fiz. 54, 612 (1968) [Sov. Phys.-JETP 27, 328 (1968)].

[8]G. M. Eliashberg, Zh. Eksp. Teor. Fiz. 55, 2443 (1968) [Sov. Phys.-JETP 28, 1298 (1969)].

[9]L. P. Gor'kov and G. M. Eliashberg, Zh. Eksp. Teor. Fiz. 55, 2430 (1968) [Sov. Phys.-JETP 28, 1291 (1969)].

[10]L. P. Gor'kov and G. M. Eliashberg, Zh. Eksp. Teor. Fiz. Pis'ma Red. 8, 329 (1968) [JETP Lett. 8, 202 (1968)].

[11]G. Lucas and M. J. Stephen, Phys. Rev. 154, 349 (1967).

[12]James W. F. Woo and Elihu Abrahams, Phys. Rev. 169, 407 (1968).

[13]Albert Schmid, Phys. Rev. 186, 420 (1969).

[14]J. T. Chen, L. G. Hayler, and Y. W. Kim, Phys. Rev. Lett 30, 645 (1973).

[15]L. G. Hayler, L. M. Geppert, J. T. Chen, and Y. W. Kim, Phys. Rev. B 11, 1924 (1975).

[16]Reiner Kümmel, *Proceedings of the International Conference on Magnetic Structures in Superconductors* (Argonne Natl. Lab., Argonne, Ill., 1973).

[17]Reiner Kümmel, Phys. Rev. B 10, 2812 (1974); and private communication.

[18]W. J. Skocpol, M. R. Beasley, and M. Tinkham, J. Low Temp. Phys. 16, 145 (1974). For a more complete list of references on voltage structures see the reference lists of this work and Ref. 15.

[19]L. M. Geppert, L. G. Hayler, J. T. Chen, and Y. W. Kim, Phys. Rev. B 14, 1062 (1976).

[20]Throughout this article we use the notation E for applied electric field and E_0 for the field inside the film.

[21]Robert Peters and Hans Meissner, Phys. Rev. Lett. 30, 965 (1973).

[22]Ivan Schuller and K. E. Gray, Phys. Rev. Lett. 36, 429 (1976).

[23]K. Maki, in Ref. 2, Chap. 18.

[24]K. Rose and M. D. Sherrill, Phys. Rev. 145, 179 (1966).

[25]T. H. K. Frederking, Chemical Engineering Progress Symposium Series, J. A. I. Ch. E. 64, 21 (1968).

[26]L. M. Geppert, T. F. Huang, and J. T. Chen (unpublished).